ALTERNATE OPERATING METHODS FOR IMPROVING THE PERFORMANCE

OF CONTINUOUS STIRRED TANK REACTORS

J. AUBIN[a]*, S.M. KRESTA[b], J. BERTRAND[a], C. XUEREB[a] and D.F. FLETCHER[c]

[a] *Laboratoire de Génie Chimique, UMR CNRS 5503, Toulouse, France*

[b] *Department of Chemical and Materials Engineering, University of Alberta, Edmonton, Alberta, Canada*

[c] *Department of Chemical Engineering, The University of Sydney, Australia*

*Corresponding author:

Dr. Joelle Aubin

Joelle.Aubin@ensiacet.fr

Laboratoire de Génie Chimique UMR CNRS 5503

5, rue Paulin Talabot, BP-1301

31106 Toulouse Cedex 01, France

ABSTRACT

The effect of the pumping direction of an axial flow impeller, the feeding rate and the number of feed inlets on the operation of a continuously-fed stirred tank has been studied using CFD. The flow patterns generated by the up-pumping and down-pumping impeller, under both 'typical' and 'intensified' operating conditions, are compared. The effect of various tank configurations on the performance of the vessel is assessed by analysing the flow and power numbers, as well as the concentration field of a non-reactive tracer. Furthermore, the inlet feed jets are reduced using traditional jet similarity analysis and are compared with that of a typical round jet. The results show that up-pumping impellers improve circulation in the upper part of the tank and reduce short-circuiting of the feed stream with only a small increase in power consumption. Furthermore, by using multiple feed inlets to increase the total throughput capacity, the amplitude of torque fluctuations is decreased and impeller bypassing is also decreased. The ensemble of conclusions suggest that the throughput capacity and mixing quality of a CSTR can be improved, without problems of short-circuiting, by employing up-pumping impellers coupled with multiple surface feed points.

INTRODUCTION

Mixing in mechanically agitated vessels is one of the most common operations encountered in the process industries. Such vessels are used for a multitude of tasks, including simple liquid blending, solids suspension, liquid-liquid emulsification, gas-liquid dispersions and chemical reactions. Often in industrial applications, agitated vessels are used in a continuous operating mode. Continuous stirred tank reactors (CSTR) have advantages over batch operation as they allow sustained high production rates, improved control and decreased operation time with the elimination of pump-out and filling stages, as well as between-cycle cleaning (Oldshue, 1983).

The performance of a CSTR is highly dependent on the hydrodynamics and turbulence levels generated in the vessel, which are determined by many factors, including the operating conditions; the agitator and vessel geometry, as well as the positions of the inlet and outlet streams. In chemical reaction applications, intense turbulence with a high rate of energy dissipation is often desired to enhance mixing at the molecular level, coupled with good convection and blending at a macro-scale to equalise the mean concentration gradients. High

throughput capacity with limited operating time and costs are important factors determining the process performance.

In a typical CSTR setup, the feed enters via the top of the tank, circulates in the vessel due to the flow generated by the impeller and then exits at the bottom. The choice of the feed flow rate in a CSTR, and thus the mean residence time ($\tau = V/Q_f$), is often related to the macromixing time, t_m, in a batch vessel. Industrially, a typical value of the ratio $\tau / t_m \sim 10$ is often employed (Mavros *et al.*, 1997; Zannoud *et al.*, 1991). For values of $\tau / t_m < 10$, short-circuiting may be likely to occur, putting at risk the performance of the reactor (Mavros *et al.*, 2002). Theoretically, submerged inlets or dip tubes which feed close to the impeller in a zone of intense turbulence are recommended for efficient mixing. Practically, however, these may generate operational problems, such as mechanical vibrations, corrosion, unwanted side reactions, and clogging (Bhattacharya and Kresta, 2004). Surface feeds are therefore often preferred. These however may be subject to mixing problems due to poor circulation and low turbulence in the upper region of the tank. This is especially true for standard batch configurations with down pumping impellers (Jaworski *et al.*, 1991; Kresta and Wood, 1993; Bittorf and Kresta, 2000, Aubin *et al.*, 2001).

In today's age where the environment and sustainable development are key issues, process improvement is a major preoccupation of industrialists. To improve the performance of CSTRs in terms of mixing and hydrodynamics, but also throughput capacity, operating time and costs, several approaches may be taken.

- If the inlet stream is fed into the tank as a high velocity 'jet', it is expected that the surrounding bulk fluid will be entrained into the feed zone, thus improving mixing, regardless of the local turbulence levels. In addition, the high inlet velocity means that the feed will be transported quickly to the impeller region where it will then be exposed to high turbulence and better mixing. Bourne and Hilber (1990) have previously shown that high feed velocities can be beneficial for fast chemical reactions in semi-batch reactors, resulting in a decrease in by-product yield. Applied to CSTRs, a high velocity feed could also be interesting for 'intensifying' the operating conditions by increasing the liquid flow rate and reducing the mean residence time, as already discussed by Mavros *et al.* (2002). However, the major difficulty associated with high velocity inlets is that the jet can pass directly through the impeller swept volume to the outlet, bypassing the majority of the tank volume and turbulent zones. To avoid this, the impeller speed has to be increased significantly.

- Up-pumping axial flow impellers have been shown to provide considerable advantages over the typical down-pumping mode and also traditional radial disc turbines, with respect to power and mixing characteristics in both single and multi phase applications (Nienow 1996, 1999; Hari-Prajitno *et al.*, 1998; Mishra *et al.* 1998; Aubin, 2001; Aubin *et al.*, 2001). In batch systems agitated by a single impeller, the up-pumping agitator generates two large circulation loops, which provide a higher circulation rate of liquid in the vessel and better turbulence characteristics, especially in the upper regions of the tank (Mishra *et al.*, 1998; Jaworski *et al.*, 2001; Aubin 2001; Aubin *et al.*, 2001, 2004). This feature is particularly interesting for surface feed applications. Bhattacharya & Kresta (2004) have recently shown that an up-pumping pitched blade turbine situated close to the liquid surface is a robust configuration for improving micromixing and thus minimizing by-product formation in cases where surface feed is required in a semi-batch tank. Another feature of up-pumping impellers is the reduced mixing times by up to 20% compared with the down-pumping operation (Aubin, 2001). Considering a time ratio $\tau / t_m \sim 10$ at a given agitation speed and feed flow rate for a standard down-pumping configuration, an up-pumping impeller operating in the same conditions will give rise to a higher time ratio due to the shorter mixing time. This suggests that the inlet flow rate of the up-pumping configuration can be increased to obtain $\tau / t_m \sim 10$, thus increasing the total throughput capacity, whilst remaining in a 'safe' operating zone.

- The location of the feed position also plays an important role in the operability of a continuously-fed stirred tank. Khopkar *et al.* (2004) have shown using CFD that by reversing the flow direction of an CSTR – inlet at the bottom and overflow type outlet – coupled with an increased rotational speed, fluid short-circuiting is reduced compared with the typical configuration.

The motivations behind this work are based on the following observations and conclusions. Firstly, it appears that in CSTRs with down-pumping impellers, short-circuiting problems are decreased when the feed flow and the impeller pumping direction are counter-current. Secondly, under intensified operating conditions, whereby the feed flow rate is increased, mixing may be promoted for surface feeds however there is a risk that the high velocity feed will pass straight through the impeller swept volume, leading to short-circuiting. Thirdly, the use of up-pumping axial flow impellers has been shown to decrease the mixing time and increase turbulence in batch reactors, as well as to lower by-product formation of reactive systems in semi-batch tanks. These observations suggest that the operating performance of a continuously fed stirred tank could be improved in one of two ways:

1. By using up-pumping axial flow impellers the mixing time decreases, which means that higher feed flow rates can be handled for the same characteristic time ratio, τ / t_m. This could then lead to decreased operating times and therefore higher throughput. Furthermore, the counter-current configuration of an up-pumping agitator and a feed inlet at the top of the tank suggests that short-circuiting problems could possibly be overcome, whilst improving mixing characteristics in the upper tank.

2. By adding a second feed inlet to the reactor, the total feed flow rate into the tank can be increased, thus intensifying the process, without the short-circuiting problems caused by a high velocity jet.

In this work, the effect of the pumping direction of an axial flow impeller, the feeding rate and the number of feed inlets on the operation of a continuously-fed stirred tank has been studied using CFD. The flow patterns generated by the up-pumping and down-pumping impeller, under both 'typical' and 'intensified' operating conditions, are compared. The operating conditions are intensified by increasing the total flow rate entering the vessel. This is done by either simply increasing the flow rate through a single inlet or by adding a second inlet. The effect of each tank configuration on the performance of the vessel is assessed by analysing the flow and power numbers, as well as the concentration field of a non-reactive tracer. Furthermore, the inlet feed jets are reduced using traditional jet similarity analysis and are compared with that of a typical round jet.

VESSEL GEOMETRY

The vessel used in this study is a cylindrical dished bottom tank ($H = T = 0.19$ m) equipped with a 3-blade axial flow Mixel TT (MTT) impeller ($D = T/2$; $C = T/3$) and four baffles ($b_w = T/10$) positioned flush against the vessel wall. The impeller is used in either the down- or up-pumping modes, designated at MTTD or MTTU, respectively. In a typical setup of the continuous mode operation, the liquid stream is introduced into the tank via a single tube with an internal diameter of 0.01 m (d_{inlet}), located midway between two adjacent baffles, 0.043 m away from the agitator shaft and the tip at 0.153 m from the vessel bottom. The outlet is 0.04m in diameter (d_{outlet}) and is situated at the centre of the bottom of the vessel. This is the same setup that has been used in previous experimental Laser Doppler Velocimetry (LDV) studies for both batch (Aubin *et al.* 2001) and continuous (Mavros *et al.* 1997) mode operation. An 'intensified' setup of the continuous mode includes a second inlet tube, which is situated directly opposite the first inlet. The apparatus is shown in Figure 1.

CFD METHOD

The numerical simulation of the flow in the vessel has been performed using ANSYS CFX5 (ANSYS, 2004) which is a general purpose commercial CFD package that solves the Navier-Stokes equations using a finite volume method and a coupled solver.

The commercial mesh generator CFX-Build was used to create a mesh composed of tetrahedral, prismatic and pyramidal elements, the latter types being generated during the mesh inflation process to increase the boundary layer resolution on walls, e.g. around the blades and on the tank walls. The mesh comprises 225 000 nodes (886 000 elements) and is shown in Figure 2. In this application, the mesh on the impeller blades was constructed from an IGES CAD file, allowing the full details, including the thickness of the blade, to be modelled. The baffles, however, are modelled as walls with zero-thickness. A preliminary grid convergence study was carried out in order to verify that the flow solution is grid independent. For this, velocities and turbulent quantities were monitored at different positions in the vessel (close to the impeller discharge and in a quiescent zone in the upper part of the tank) and the results of three different grid sizes were compared.

A no-slip boundary condition is imposed on the agitator blades, baffles and vessel walls. The rotational speed of the impeller, N, was 3 Hz, which corresponds to a Reynolds number of 27 000. Water at 25 °C and 1 atm is used as the operating fluid and the free liquid surface is modelled with a zero-flux and zero-stress condition applied. The boundary condition at the feed inlet(s) was a mass flow rate, Q_f. A flow rate of 1.068×10^{-1} kg.s^{-1} (6.4 Lmin^{-1}) was compared with an intensified total flow rate of 1.931×10^{-1} kg.s^{-1} (11.6 Lmin^{-1}). The intensified flow rate enters the vessel via one inlet at 1.931×10^{-1} kg.s^{-1} or two inlets with 0.966×10^{-1} kg.s^{-1} in each for an equal intensified total flowrate. The corresponding time ratios (τ / t_m), feed Reynolds numbers (Re_f), and macromixing characteristics are given in Table 1. At the outlet, a constant average pressure condition ($P_{ave} = 0$) was imposed. After convergence of the turbulent flow field, a non-reacting scalar was added at the inlet in order to observe the mixing of two species.

In a baffled stirred tank under turbulent conditions, baffle-impeller interactions exist which cause a periodic, time-dependent flow. When the tank is operating in the continuous mode, the feed inlet also causes a time dependent flow. Such interactions necessitate the use of a modelling approach for several moving zones, such as the sliding mesh model (Luo *et al.*, 1993) or the multiple reference frames method (Luo *et al.*, 1994). In order to simulate the mixing of two species as a function of time in the continuous flow vessel, the sliding mesh model was required. The interface between the rotating and stationary zones was positioned at mid-distance between the impeller and the vessel wall, and just above and below the impeller swept volume. The mesh was

refined in the rotating zone, as can be seen in Figure 2. A time step equal to 5×10^{-3} s was used, which corresponds to an impeller rotation of 5.4 °.

The CFX5.6 solver was used to solve the momentum, continuity and turbulence equations for the fluid flow in the vessel. The turbulence model used is the well known standard k-ε model with standard wall functions. The advection terms in each equation were discretized using a bounded second order differencing scheme. Simulations were typically considered converged when the normalised residuals for the velocities and turbulence quantities fell below 10^{-4} and when the mean power number was stable. This was achieved after approximately 20 impeller revolutions with, in general, 4 internal iterations for each time step

RESULTS AND DISCUSSION

The first part of this section describes the effect of the feed on the hydrodynamics in the vessel and on the global operating characteristics of the impeller for the various CSTR configurations, and compares them with batch operation. Secondly, the mixing quality of the diverse configurations is assessed via the analysis of tracer dispersion in the tank. Finally, the inlet feed jets are reduced using turbulent jet theory and are compared with a free round jet. The aim is to determine the extent to which jet theory is applicable to the feed streams, as well as the influence of the recirculating flow surrounding the jet and the possible interactions between two jets.

Hydrodynamics and Global Impeller Characteristics

Down-pumping configurations

Figures 3 (a-f) show the radial-axial flow patterns generated in the various CSTR configurations with the down-pumping impeller and compares them with the equivalent batch stirred tank (Figure 3 (g)). The vector plots shown correspond to mean velocity fields, mid-way between two baffles, which have been averaged over the angular rotation of the impeller. For all cases, the impeller forms a primary circulation loop in the lower half of the vessel, flowing upwards at the wall, regardless of the inlet flow rate or the number of inlets. For the configurations with a single feed point, however, the flow patterns are not symmetric: it can be seen in the upper corner of the vessel, furthest from the feed, that the circulation is minimal and is not much different from the batch case. Furthermore, in these cases, the regularity of the secondary circulation loop below the impeller appears to be lost. With two feed inlets, however, the bulk flow patterns are much more symmetrical and circulation is induced close to the liquid surface, particularly in the plane at 90° to the feed.

The level of bypassing occurring when an impeller blade is directly beneath the inlet is assessed by evaluating the mean down-flowing axial flow, $\overline{U}_{neg}$, and its standard deviation in the horizontal plane 3 mm below the impeller swept volume (Table 2). It is not surprising that when the feed flow rate using one inlet increases, the mean down-flowing axial flow, $\overline{U}_{neg}$, and its standard deviation also increases. This increase in the standard deviation signifies a divergence from uniform downward flow below the impeller, therefore suggesting possible short-circuiting. When the feed flow is increased by adding a second inlet ($\tau/t_m = 3.76$), there is only a slight increase in the downward flow due to the fact that the second inlet enters between two blades, however the standard deviation remains the same as when $\tau/t_m = 6.80$.

The impeller flow number, Fl, and mean power number, $\overline{P}_o$ are also presented in Table 2. Additionally, for the batch cases, the experimental values that have been reported in the literature (Mavros *et al*., 1996; Baudou, 1997; Aubin *et al*., 2001) for the same vessel are also tabulated. The calculated values of both $\overline{P}_o$ and Fl are in general agreement with these experimental data, which supports the simulations. Nevertheless, the difficulty of obtaining these data is shown with the range of values given by the three experimental studies, all of which were carried out in the same vessel but by different experimentalists and with sometimes different measuring equipment. In addition, small differences in the simulated impeller geometry compared with real impeller and its inherent imperfections (e.g. due to manufacturing techniques) can lead to variations in the power consumption, as discussed by Chapple et al. (2002). Concerning the impeller flow number, it can be seen that as the feed inlet velocity increases ($\tau/t_m = 3.76$, 2 inlets $\rightarrow$ $\tau/t_m = 6.80$ $\rightarrow$ $\tau/t_m = 3.76$), Fl also increases. It is interesting to point out that with a high feed rate ($\tau/t_m = 3.76$) and two inlets, Fl is not much different than for batch operation. This suggests that minimal impeller bypassing occurs when the tank throughput is increased using two inlets. Comparison of mean power number, $\overline{P}_o$, for the various configurations shows that there is little effect of the feed on this parameter. However, it is interesting to consider the effect of the position of the impeller blades with respect to the position of the feed inlet. Figure 4 shows the power number, P_o, as a function of the relative impeller blade – feed inlet position. The reference value of 0° is where an impeller blade is directly beneath the feed inlet. Looking at the filled symbols in Figure 4, it can be seen that P_o oscillates in a sinusoidal manner with a minimum when the impeller blade is directly beneath the feed inlet. The amplitude increases with the feed inlet velocity and the frequency is equal to the product of the rotational speed, the number of blades and the number of feed inlets, i.e. $f = N \times N_b \times N_i$.

Up-pumping configurations

The radial-axial circulation patterns in the feed plane and at 90° to the feed plane for the up-pumping cases are presented in Figures 5 (a-f), and are compared with the flow pattern of the equivalent batch operation (Figure 5 (g)). Like for the down-pumping results, the vector plots shown correspond to mean velocity fields, mid-way between two baffles, which have been averaged over the angular rotation of the impeller. For the cases with a single feed inlet (Figures 5 (a-d)), the upward impeller discharge stream is at 45° towards the tank wall. When this jet impinges on the wall, it separates into two, forming a clearly defined circulation loop in the upper part of the tank, which is similar to the flow patterns in the batch configuration. Below the impeller, however, the circulation pattern is extremely irregular. When two inlets feed the vessel (Figures 5 (e-f)), the regular upper circulation loops are completely disrupted, giving rise to an irregular flow pattern throughout the tank.

The lower half of Table 2 shows the mean down-flowing axial flow and its standard deviation below the impeller for the up-pumping cases when an impeller blade is directly below the feed inlet. For the case where $\tau / t_m = 8.13$, there is almost no downward flow at the lower impeller plane, implying no short-circuiting. When the feed flow rate is increased using one or two inlets, the down flow velocities and standard deviations are slightly higher, which is expected. However, for all configurations, these values are significantly lower than those for the equivalent down-pumping cases. As a result, since the MTTU removes the down flow, it is harder for the feed stream to get to the outlet and thus short-circuiting may be reduced.

The effect of the various configurations on Fl and $\overline{P_o}$ are also shown in the lower part of Table 2. For all cases, the value of Fl is very similar to that of the batch tank. A slight decrease in Fl is observed for $\tau / t_m = 8.13$; this may be because the inlet jet counteracts the impeller discharge, thus reducing the pumping capacity. When the flow rate is increased using one inlet ($\tau / t_m = 4.50$), Fl increases slightly. This is most probably not an increase in pumping capacity but rather an increase in the flow discharge from the impeller swept volume due to the fact that the inlet jet has more of a tendency to pass through the impeller. Whilst the down-pumping configurations had no significant effect on the mean power consumption, $\overline{P_o}$ for the up-pumping cases increases with increasing feed velocity ($\tau / t_m = 4.50$, 2 inlets → $\tau / t_m = 8.13$ → $\tau / t_m = 4.50$). In addition, P_o for the up-pumping configurations is generally higher than for the down-pumping impellers (0.6-1.1 vs 0.5 to 0.7) and the fluctuations of P_o as a function of the relative impeller blade – feed inlet position are more important (Figure 4, open symbols). The amplitude of these oscillations increases with increasing feed velocity and is dependent on both the number of impeller blades and inlets, as for the down-pumping cases. Such P_o fluctuations

are important to consider when designing the processes: high amplitude oscillations can rapidly lead to the deterioration of the agitator, shaft and motor.

Mixing Analysis using a Non-Reactive Tracer

The mixing performance of the various CSTR configurations is assessed by simulating the convection and turbulent diffusion of a non-reactive tracer feed. The concentration fields, as well as the mean tracer concentration and corresponding standard deviation, σ, after 10s of mixing are depicted in Figures 6 and 7, for the down- and up-pumping cases, respectively. For all cases, the concentration fields in the feed plane and normal to the feed plane are highly asymmetric and clearly emphasize the three dimensionality of the mixing field. The authors wish to point out, however, that the exact numerical values of the tracer dispersion should be taken with caution. It is well known that the use of RANS equations for modelling turbulence in stirred tanks does not allow the correct estimation of the turbulence quantities. As a result, the turbulent dispersion is also incorrectly estimated, which directly affects tracer concentration. Nevertheless, the calculated concentration fields are useful for the qualitative comparison of different configurations and for understanding the uniformity of tracer dispersion as done here.

The deviation from uniformity of the tracer dispersion is assessed by the standard deviation of the mean concentration in the vessel. For all cases, except the high feed rate with the down-pumping impeller ($\tau / t_m = 3.76$), the mixing quality is relatively similar with values of σ in the range 0.052-0.067. For the down-pumping case with $\tau / t_m = 3.76$, however, $\sigma = 0.103$, which suggests significantly poorer mixing.

Analysis of the Feed Jet

Considering the velocity, U_f, and Reynolds number, Re_f, of the various feed streams studied in this work (Table 1), the feed inlet is expected to possess features similar to those of a fully turbulent jet. However, the behaviour of the feed is also expected to deviate from that of a free jet due to the confined geometry of the surrounding tank, as well as the complex three dimensional flow field induced by the impeller. In this section, the feed jet in the CSTR is reduced using classical turbulent jet theory and compared with the behaviour of a free circular jet.

The behaviour of axisymmetric turbulent jets has been studied extensively (see for example, Rajaratnam (1976) and Pope (2000)) and is therefore well understood. Close to the inlet, the jet flows with an undiminished velocity equal to U_{core} (= U_f). Further away from the inlet, the jet gradually starts to slow down and spread out radially. At any axial distance from the inlet, z, the maximum axial velocity, U_m, is at the centreline, and

decreases in the radial direction. The jet half-width, b, corresponds to the radial distance, r, from the centreline of the inlet where the axial velocity, U, equals $U_m/2$. In addition, the radial profiles of the axial velocity at different axial locations collapse onto a single curve when U is scaled with U_m and r is scaled with b ($\eta = r / b$). For circular jets, the decay in the jet velocity is inversely proportional to the distance from the inlet, whilst the jet expands linearly as it moves away from the inlet (Rajaratnam, 1976). Having compared both the Tollmien and Goertler solutions with experimental data, Rajaratnam (1976) suggests the following equations for the jet expansion and velocity decay for the turbulent round jet:

$$b = C_2 \left(z - z_o \right) \tag{1}$$

$$\frac{U_m}{U_{core}} = 6.3 \frac{d_{inlet}}{\left(z - z_o \right)} \tag{2}$$

where C_2 is a constant equal to 0.10, d_{inlet} is the diameter of the feed inlet and z_o is the virtual origin of the jet.

Similarity profiles

Figure 8 shows the similarity profiles of the feed jet velocity for the various configurations of the CSTR compared with the Goertler solution for a free circular jet (Rajaratnam, 1976). For all graphs, the velocity profiles correspond to a relative impeller blade – inlet position of 0° (i.e. the impeller blade is positioned directly beneath the inlet), unless stated otherwise. This position is expected to create the highest amount of interaction between the feed jet and the surrounding flow.

For the lower feed rates, Figures 8 (a, b), it can be seen that the velocity profiles are self-similar for the range $-1.0 < \eta < 1.0$ and correspond very well with the solution for a free turbulent jet. In addition, the flow patterns created by the impeller, regardless of the pumping direction, do not influence the similarity of the velocity profiles. When the feed flow rate is increased, Figures 8 (c, d), two distinguishing features are observed. Firstly, the range of self-similarity is extended to almost $-2.0 < \eta < 2.0$; secondly, the centreline of the velocity profile is shifted towards the tank wall (i.e. towards $\eta > 0$), due to the tangential flow induced by the impeller. In addition, it appears that the similarity profiles of the feed jet are not affected by the pumping direction of the impeller. When the feed enters via two inlets, the profiles for down- and up-pumping configurations (Figures 8 (e-h)) are quite different. For the down-pumping configuration, Figures 8 (e, g), self-similarity is conserved for the range $-1.0 < \eta < 1.0$ for both feed streams. For the feed stream that enters between two blades, the similarity profiles are in very good agreement with the solution for a free circular jet. For the feed positioned over the

blade, however, the centreline of the profile is shifted towards the outer part of the tank, as observed in Figures 8 (c, d). For the up-pumping case, when the feed enters between two blades, self-similarity is conserved for $-1.0 < \eta < 1.0$, although the centreline of the velocity profiles shifts slightly towards the outer tank. When the inlet is positioned over the blade, however, self-similarity is completely lost. As the jet travels away from the inlet, the centreline of the scaled velocity profiles moves further and further towards the vessel wall. This feature suggests that the jet is influenced significantly by the second feed stream, the blade position and the impeller pumping direction.

Overall, these results show that the behaviour of the feed jet in the CSTR is quite similar to that of a turbulent circular jet in unconfined conditions. In general, the jet appears to be only slightly influenced by the surrounding tangential flow field, irrespective of the impeller pumping direction. The feed jet only deviates strongly from classical behaviour in the particular conditions of the up-pumping configuration with two inlets.

Jet expansion and velocity decay

The virtual origin of the jet and the constant C_2 (rate of jet expansion) for the various CSTR configurations are given in Table 3. C_2 is determined by calculating the slope of the linear curve 'b *versus* z'; z_o is the value of z when b = 0. For all cases, the value of C_2 is in the range 0.07–0.11, which agrees well with the value of 0.10 for the free round jet (Rajaratnam, 1976). The virtual origin of the jet is situated in the range $5.1d_{inlet}$–$6.6d_{inlet}$ upstream from the feed inlet for the down-pumping cases, and a bit further from the inlet ($5.8d_{inlet}$–$7.6d_{inlet}$) for the up-pumping configurations. Note that the virtual origin is different for each configuration, which suggests that this parameter is not only dependent on the vessel geometry, but also the feed velocity.

The expansion of the feed stream jet until the top boundary of the impeller swept volume for the various down- and up-pumping configurations is presented in Figures 9 (a) and (b), respectively. The results are compared with equation [1] given by Rajaratnam (1976) for a turbulent round jet. Note that since z_o is different for each configuration, $(z - z_o) / d_{inlet}$ is also different for each configuration at a particular axial distance from the inlet (z). To help understanding, a box has been drawn around the point taken at a fixed distance from the inlet, on the top boundary of the impeller swept plane.

For the down pumping cases, the behaviour of the feed jet is very similar to that of a circular jet, although the expansion rate is slightly slower. This is most probably due to the circulation patterns of the surrounding liquid in the tank. Several features of the jet expansion in the up-pumping configurations are worth noting. For the cases with one feed inlet, the jet expands at a slower rate than the down-pumping configurations

and the circular jet. With two feed inlets, the stream entering between two blades behaves like a traditional round jet until close to the impeller swept plane. On the other hand, the stream entering directly over the blade deviates from classical behaviour relatively close to the feeding location. These results again show the strong interaction between the feed jet behaviour, the impeller blade position and the hydrodynamics in this vessel.

The decay of the maximum axial velocity at different positions from the inlet for the various configurations is shown in Figures 9 (c) and (d). For both the down- and up-pumping cases, two distinct regions can be identified, corresponding to the jet decay region and the deflection of the jet due to the presence of the rotating impeller. For the down-pumping cases, the decay of the feed stream is in relatively good agreement with that of a circular jet (equation [2]), despite the surrounding fluid circulation. The agreement is best at a higher flow rate and also when the jet is not positioned over a blade. For the up-pumping configurations, the jet decay deviates from that of a round jet, which is not at all surprising. When the feed enters via one inlet, the decay in the deflection region is much faster than for the down-pumping configurations, clearly a result of the circulation patterns induced by the up-pumping impeller. In addition, the deflection of the jet occurs closer to the feed point than with the down-pumping configurations. This is consistent with the similarity profiles and jet expansion, suggesting disintegration of the feed jet well before it reaches the impeller swept volume.

CONCLUSIONS

In this work we have used CFD to study the effect of the pumping direction of an axial flow impeller, the feed rate and the number of feed inlets on the operation of a continuously-fed stirred tank, with the aim of finding alternate operating methods for improving the operating performance. The circulation patterns and tracer concentration fields created under the various operating conditions and geometries have been assessed, and the impeller performance has been analysed. In addition the behaviour of the feed jet has been characterised using traditional jet analysis and compared with that of a turbulent round jet.

The main conclusions are as follows.

- The CSTRs with a down-pumping impeller and one feed inlet are characterised by poor circulation in the upper part of the tank. The addition of a second feed inlet improves the circulation in this region. On the other hand, circulation is further improved when the CSTR is stirred by an up-pumping impeller. Furthermore, feed short-circuiting through a bottom outlet may be reduced when the impeller is used in the up-pumping mode.

- The power number of the impeller fluctuates as a function of the rate of blade passage and the number of inlets. The amplitude of these fluctuations increases with increasing feed velocity.

- The concentration fields of the CSTRs are highly three dimensional and uniform mixing is more likely to be obtained using up-pumping impellers or with down-pumping impellers and lower feed rates.

- The feed jet in the CSTR has been shown to have similar behaviour to that of a turbulent circular jet in unconfined conditions. In general, the jet appears to be only slightly influenced by the surrounding tangential flow field, irrespective of the impeller pumping direction. As expected, the feed jet is less affected by the down-pumping impeller than by the up-pumping impeller.

Overall, the ensemble of these conclusions suggest that the throughput capacity and mixing quality of a CSTR can be improved, without problems of short-circuiting, by employing up-pumping impellers coupled with multiple surface feed points. By using two (or more) feed points the inlet velocity can be decreased whilst maintaining a sufficient through put. A greater the number of feed points results in a smaller amplitude of the P_o fluctuations and a feed jet velocity that decays more rapidly, which improves the mixing quality in the tank.

Future work will investigate experimentally the effect of various configurations on micromixing efficiency via the study of competing-parallel reactions.

NOTATION

b	Jet half-width (m)
b_w	Baffle width (m)
C	Distance of impeller from vessel base (m)
C^*	Volume fraction of the tracer concentration (−)
$\overline{C^*}$	Average volume fraction of the tracer concentration (−)
C_2	Constant (−)
d_{inlet}	Feed inlet diameter (m)
D	Impeller diameter (m)
f	Frequency (s^{-1})
Fl	Flow number, $\dfrac{Q_{Fl}}{ND^3}$ (−)
H	Vessel height (m)
k	Turbulent kinetic energy (m^{2}s^2)
MTTD	Down-pumping Mixel TT
MTTU	Up-pumping Mixel TT
N	Impeller rotation speed (s^{-1})
N_b	Number of impeller blades (−)
N_i	Number of feed inlets (−)
P	Power consumption, $2\pi\,N\,T_o$ (W)
$\overline{P}$	Time averaged power consumption, $2\pi\,N\,\overline{T_o}$ (W)
P_{ave}	Average pressure (Pa)
P_o	Power number, $\dfrac{P}{\rho\,N^3 D^5}$ (−)
$\overline{P_o}$	Time averaged power number, $\dfrac{\overline{P}}{\rho\,N^3 D^5}$ (−)
Q_f	Feed flow rate (m^{3}s^{-1})
Q_{Fl}	Impeller pumping capacity (m^{3}s^{-1})
r	radial distance from the centre of the inlet (m)

Re	Impeller Reynolds number, $\dfrac{\rho\,ND}{\mu}$ (−)
Re$_f$	Feed Reynolds number, $\dfrac{\rho\,U_f\,d_{inlet}}{\mu}$ (−)
T	Vessel diameter (m)
T$_o$	Torque (N m)
$\overline{T_o}$	Time averaged torque (N m)
t_c	Circulation time (s)
t_m	Mixing time (s)
U	Axial velocity of the jet (m s^{-1})
U$_{core}$	Core velocity of the jet (= U$_f$) (m s^{-1})
U$_f$	Feed velocity (= U$_{core}$) (m s^{-1})
U$_m$	Local maximum velocity of the jet (m s^{-1})
z	Axial distance from the inlet (m)
z$_o$	Virtual origin of the jet (m)

Greek Symbols

ε	Dissipation of turbulent kinetic energy (m^{2}s^3)
η	Dimensionless radial distance, r / b (−)
μ	Viscosity (Pa s)
ρ	Density (kg m^{-3})
σ	Standard deviation
τ	Mean residence time, V/Q$_f$ (s)

REFERENCES

ANSYS, 2004, ANSYS CFX5.6, ANSYS Europe, Gemini Building, Harwell, Didcot, Oxfordshire, UK. See also www.ansys.com/cfx.

Aubin, J., 2001, *Mixing capabilities of down- and up-pumping axial flow impellers in single phase and gas-liquid systems: experimental and CFD studies*, PhD Thesis, INPT France and The University of Sydney Australia.

Aubin, J., Mavros, P., Fletcher, D.F., Bertrand, J., and Xuereb, C., 2001, Effect of axial agitator configuration (up-pumping, down-pumping, reverse rotation) on flow patterns generated in stirred vessels, *Chem Eng Res Des*, 79(A): 845-856.

Aubin J., Le Sauze, N., Bertrand, J., Fletcher, D.F. and Xuereb, C., 2004, PIV measurements of flow in an aerated tank stirred by a down- and an up-pumping axial flow impeller, *Exp. Therm. Fluid Sci.*, 28(5), 447-456.

Baudou, C., 1997, *Agitation par des systèmes axiaux simples ou multi-etagés. Obtention de l'hydrodynamique par vélocimétrie laser à effet doppler*, Ph.D. Thesis (INP Toulouse, France).

Bittorf, K.J. and Kresta, S.M, 2000, Active volume of mean circulation for stirred tanks agitated with axial impellers, *Chem. Eng. Sci.*, 55(7), 1325-1335.

Bhattacharya, S. and Kresta, S.M., 2004, Surface feed with minimum by-product formation for competitive reactions, *Chem Eng Res Des*, 82(A): 1153-1160.

Bourne J.R. and Hilber C.P, 1990, The productivity of micromixing-controlled reactions: effect of feed distribution in stirred tanks, *Chem Eng Res Des*, 68(A): 51-56.

Chapple, D., Kresta, S.M., Wall, A. and Afacan, A., 2002, The effect of impeller and tank geometry on power number for a pitched blade turbine, *Chem Eng Res Des*, 80(A): 364-372.

Hari-Prajitno, D., Mishra V.P., Takenaka, K., Bujalski, W., Nienow, A.W., and McKemmie, J., 1998, Gas-liquid mixing studies with multiple up-and down-pumping hydrofoil impellers: power characteristics and mixing time, *Can. J. Chem. Eng.*, 76(10), 1056-1068.

Jaworski, Z., Nienow, A.W., Koustsakos, E., Dyster, K. and Bujalski, W., 1991, An LDA study of turbulent flow in a baffled vessel agitated by a pitched blade turbine, *Chem Eng Res Des*, 69(A): 313-320.

Jaworski, Z. Dyster, K.N. and Nienow, A.W., 2001, The effect of size, location and pumping direction of pitched blade tubine impellers on flow patterns: LDA measurements and CFD predictions, *Chem Eng Res Des*, 79(A), 887-894.

Khopkar, A.R., Mavros., P. Ranade, V.V. and Bertrand, J., 2004, Simulation of flow generated by an axial-flow impeller: batch and continuous operation, *Chem Eng Res Des,* 82(A): 737-751.

Kresta, S.M. and Wood, P.E., 1993, The mean flow field produced by a 45° pitched blade turbine: changes in circulation pattern due to off bottom clearance, *Can. J. Chem. Eng*., 71, 45-53.

Luo, J.Y., Gosman, A.D., Issa, R.I., Middleton, J.C. and Fitzgerald, M.K., 1993, Full flow field computation of mixing in baffled stirred vessels, *Chem Eng Res Des,* 71(A): 342-344.

Luo, J.Y., Issa, R.I. and Gosman, A.D., 1994, Prediction of impeller-induced flows in mixing vessels using multiple frames of reference, *8th European Conf. on Mixing, Cambridge*, 138, *IChemE Symposium*, 549.

Mavros, P., Xuereb, C. and Bertrand, J., 1996, Determination of 3-D flow fields in agitated vessels by laser Doppler velocimetry: Effect of impeller type and liquid viscosity on liquid flow patterns, *Chem Eng Res Des*, 74(A): 658-668.

Mavros, P., Naude, I., Xuereb, C., and Bertrand, J., 1997, Laser Doppler Velocimetry in agitated vessels: effect of continuous liquid stream on flow patterns, *Chem Eng Res Des*, 75(A): 763-776.

Mavros, P., Xuereb, C., Fort, I. and Bertrand, J., 2002, Investigation by Laser Doppler Velocimetry of the effects of liquid flow rates and feed positions on the flow patterns induced in a stirred tank by an axial-flow impeller, *Chem Eng Sci*, 57, 3939-3952.

Mishra, V.P., Dyster, K.N., Jaworski, Z., Nienow, A.W., and McKemmie, J., 1998, A study of an up- and a down-pumping wide blade hydrofoil impeller; Part I. LDA measurements, *Can. J. Chem. Eng*., 76, 577-588.

Nienow, A.W., 1996, Gas-liquid mixing studies: A comparison of Rushton turbines with some modern impellers, *Chem Eng Res Des*, 74(A): 417-423.

Nienow, A.W., 1999, The versatility of up-pumping wide-blade hydrofoil agitators, Proc. *3rd Inter. Symp. on Mixing In Industrial Processes*, Osaka, Japan, 173-180.

Oldshue, J.Y., 1983, *Fluid mixing technology*, McGraw-Hill Pub. Co., New York, NY.

Rajaratnam, N., 1976, *Developments in Water Science: Turbulent Jets*, Elsevier Scientific Publishing Co., New York, NY.

Pope, S.B., 2000, *Turbulent Flows*, Cambridge University Press, Cambridge, UK.

Zannoud, N., Giraud, P., Costes, J. and Bertrand, J., 1991, Local laser measurements of velocities and concentration in two continuous systems: A tubular jet-stirred reactor and a stirred vessel, *Proceedings of 7th European Conf. on Mixing*, Brugge, 18-20 Sept, 173-180, Antwerpen: EFCE-KVIV.

List of Tables

Table 1: Process and macromixing characteristics of the CSTR configurations.

Table 2: Comparison of the global impeller characteristics of the various CSTR configurations.

Table 3: Rate of jet expansion, C_2, and the virtual origin for the various CSTR configurations investigated.

Configuration	Process Characteristics				Macromixing Characteristics	
	Total feed rate Q_f (m^3.s^{-1})	Feed inlet velocity U_f (m.s^{-1})	Reynolds at feed inlet(s) Re_f	Time ratio τ / t_m	Mixing time t_m (s)	Circulation time t_c (s)
MTTD (1 inlet)	1.068×10^{-4}	1.36	1.36×10^4	6.80		
MTTD (1 inlet)	1.931×10^{-4}	2.46	2.46×10^4	3.76	7.47[1]	1.85[1]
MTTD (2 inlets)	1.931×10^{-4}	1.23	1.23×10^4	3.76		
MTTU (1 inlet)	1.068×10^{-4}	1.36	1.36×10^4	8.13		
MTTU (1 inlet)	1.931×10^{-4}	2.46	2.46×10^4	4.50	6.00[1]	1.55[1]
MTTU (2 inlets)	1.931×10^{-4}	1.23	1.23×10^4	4.50		

[1] Experimental values for batch systems reported by Aubin (2001).

Table 1

Case	Power Number, P_o	Flow Number, Fl	Lower Impeller Plane (3 mm below C)	
			$\overline{U}_{neg}$ (m/s)	Std deviation $\overline{U}_{neg}$
MTTD $\tau / t_m = 6.80$	0.59	0.80	-0.220	0.086
MTTD $\tau / t_m = 3.76$	0.58	0.88	-0.295	0.711
MTTD 2 inlets, $\tau/ t_m = 3.76$	0.55	0.70	-0.247	0.086
MTTD Batch	0.58 (0.65[a], 0.60[b], 0.74[c])*	0.66 (0.74[a], 0.63[b], 0.67[c])*	—	—
MTTU $\tau / t_m = 8.13$	0.77	0.64	-0.001	0.006
MTTU $\tau / t_m = 4.50$	0.88	0.73	-0.073	0.216
MTTU 2 inlets, $\tau/ t_m = 4.50$	0.70	0.69	-0.017	0.073
MTTU Batch	0.65 (0.67[c])*	0.69 (0.61[c])*	—	—

*Experimental values given by [a]Mavros *et al*. (1996), [b]Baudou (1997) and [c]Aubin et al. (2001).

Table 2

Case	Constant, C_2	Virtual Origin, z_o (m)
MTTD $\tau / t_m = 6.80$	0.08	-0.066
MTTD $\tau / t_m = 3.76$	0.09	-0.058
MTTD 2 inlets, $\tau / t_m = 3.76$, (inlet over blade)	0.11	-0.051
MTTD 2 inlets, $\tau / t_m = 3.76$, (inlet between blades)	0.08	-0.065
MTTU $\tau / t_m = 8.13$	0.07	-0.076
MTTU $\tau / t_m = 4.50$	0.08	-0.066
MTTU 2 inlets, $\tau / t_m = 4.50$, (inlet over blade)	0.10	-0.058
MTTU 2 inlets, $\tau / t_m = 4.50$, (inlet between blades)	0.09	-0.057

Table 3

List of Figures

Figure 1: Schematic diagram of the vessel geometry.

Figure 2: Radial cross section of the mesh used for the CFD simulations.

Figure 3: Vector plots for the various operating conditions and tank configurations with the MTTD.

Figure 4: Vector plots for the various operating conditions and tank configurations with the MTTU.

Figure 5: Evolution of the power number, P_o, with the position of the impeller blade relative to the feed point. At $0°$ an impeller blade is directly beneath the feed inlet.

Figure 6: Concentration fields of the tracer after 10s. Various operating conditions and tank configurations with the MTTD.

Figure 7: Concentration fields of the tracer after 10s. Various operating conditions and tank configurations with the MTTU.

Figure 8: Effect of the feed flow rate, the number of inlets and the impeller pumping direction on the similarity profiles. $\eta = 0$ is the centerline of the inlet, $\eta < 0$ is towards the impeller shaft and $\eta > 0$ is towards the tank wall.

Figure 9: Expansion of the jet half-width (a-b) and the decay of maximum velocity (c-d) for the various CSTR configurations as a function of axial distance from the feed inlet. The first point for each series is situated immediately after the inlet. The last point (with a box around it) is at the top boundary of the impeller swept volume. Note that the initial radius of the jet is 0.05m.

Inlets

Baffles

Baffles

Outlet
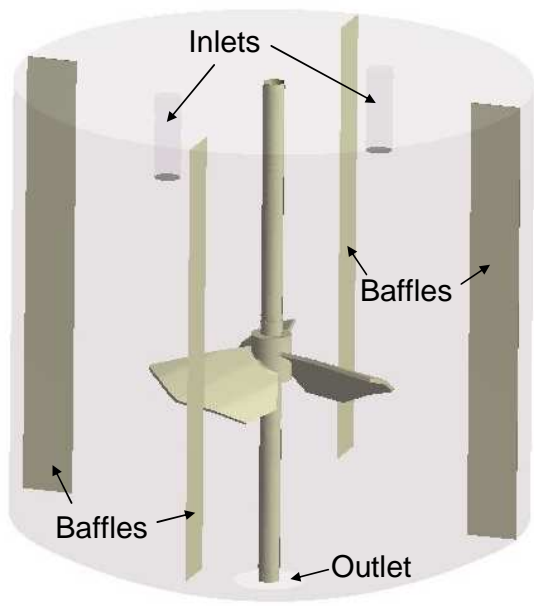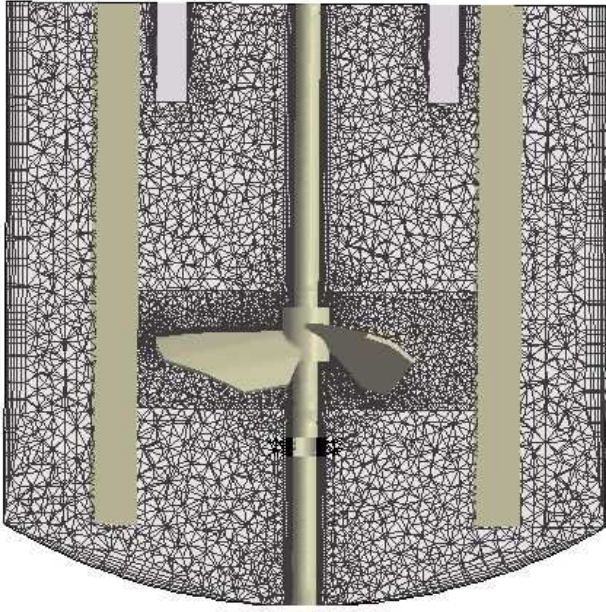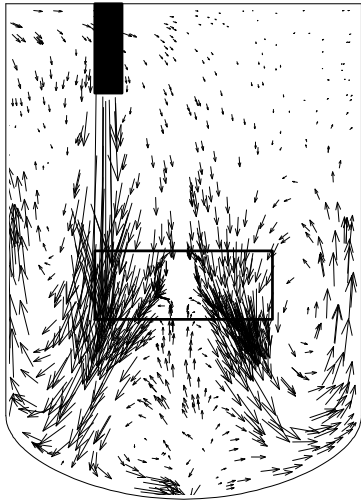
Figure 1

Figure 2

(a) MTTD, $\tau / t_m = 6.80$
Feeding-tube plane
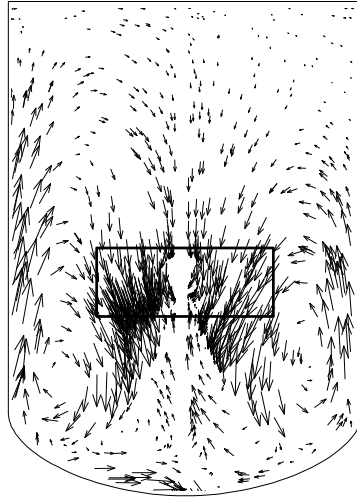
(b) MTTD, $\tau / t_m = 6.80$
90°-rotated plane
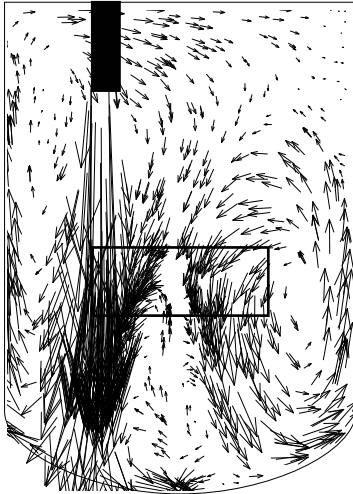
(c) MTTD, $\tau / t_m = 3.76$
Feeding-tube plane
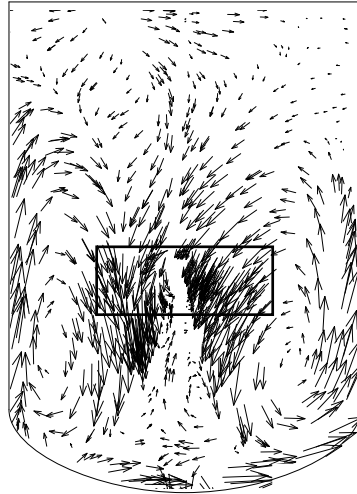
(d) MTTD, $\tau / t_m = 3.76$
90°-rotated plane

(g) MTTD, batch

0.5 Vtip
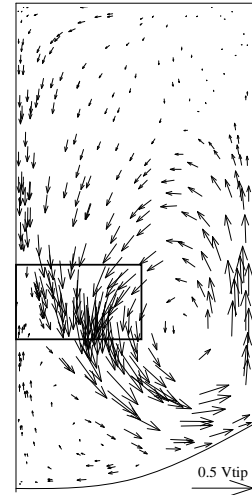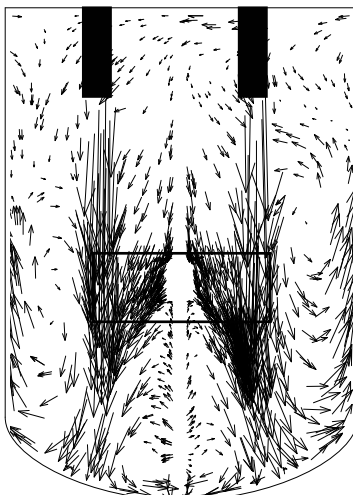
(e) MTTD (2 inlets), $\tau / t_m = 3.76$
Feeding-tube plane
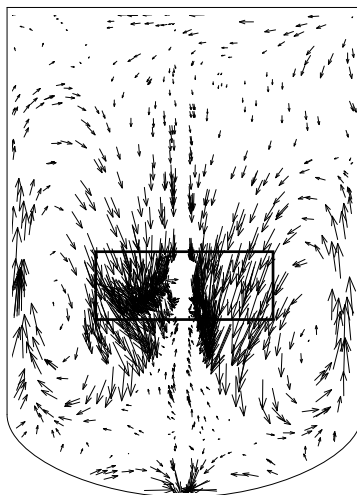
(f) MTTD (2 inlets), $\tau / t_m = 3.76$
90°-rotated plane

Figure 3
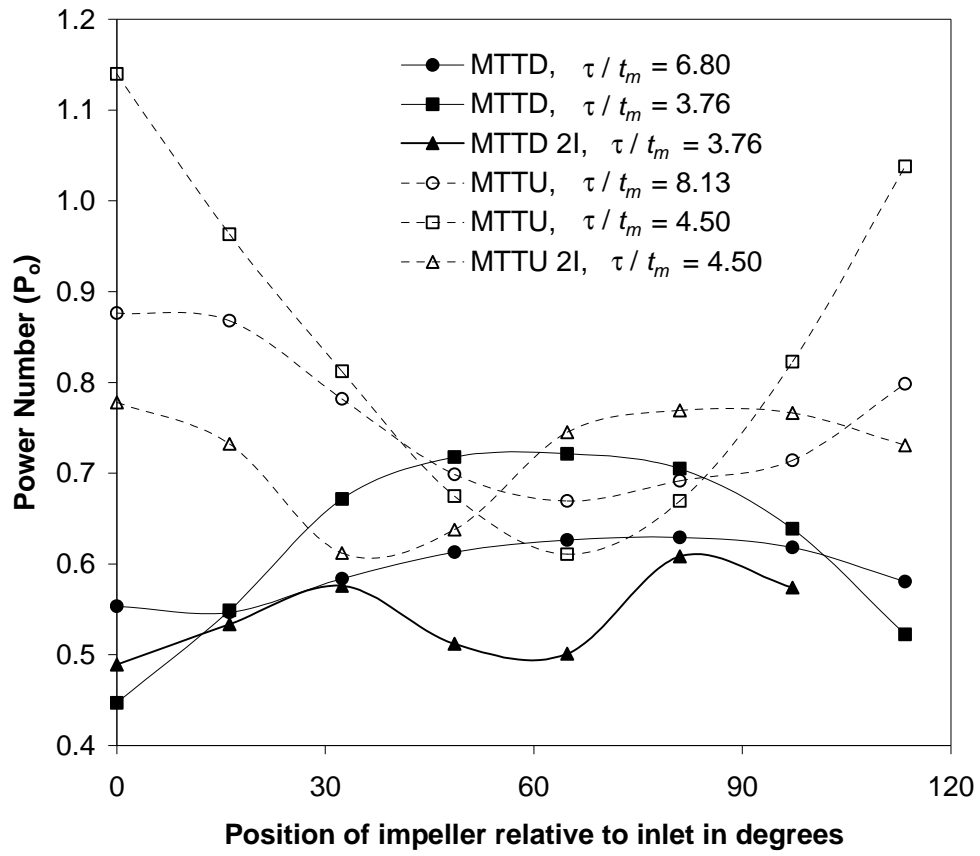
Figure 4
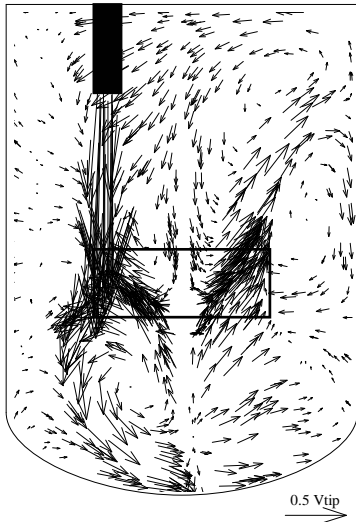
(a) MTTU, $\tau / t_m = 8.13$
Feeding-tube plane
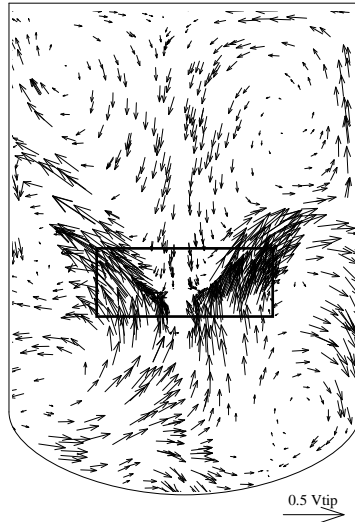
(b) MTTD, $\tau / t_m = 8.13$
90°-rotated plane
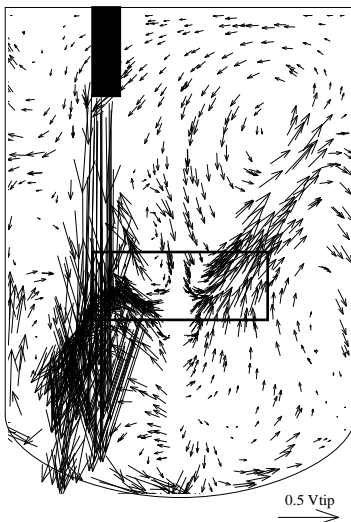
(c) MTTU, $\tau / t_m = 4.50$
Feeding-tube plane
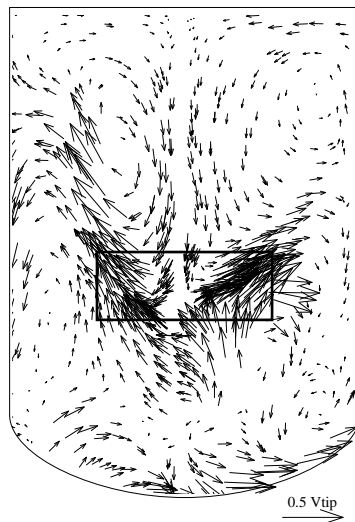
(d) MTTU, $\tau / t_m = 4.50$
90°-rotated plane
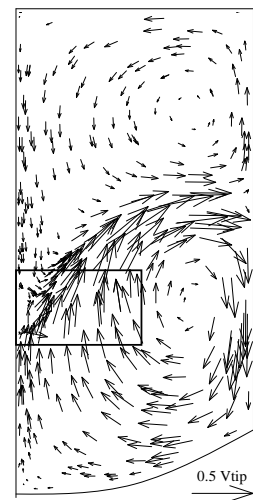
(g) MTTU, batch
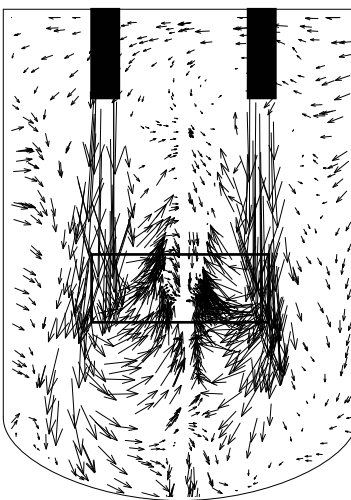
(e) MTTU (2inlets), $\tau / t_m = 4.50$
Feeding-tube plane
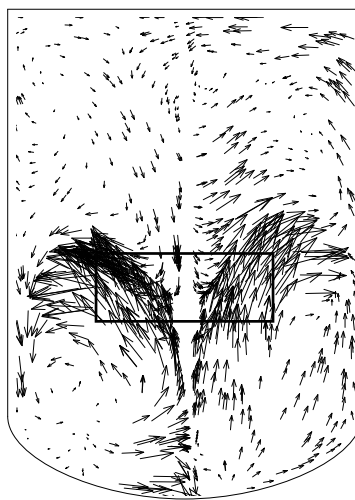
(f) MTTU (2 inlets), $\tau / t_m = 4.50$
90°-rotated plane

Figure 5
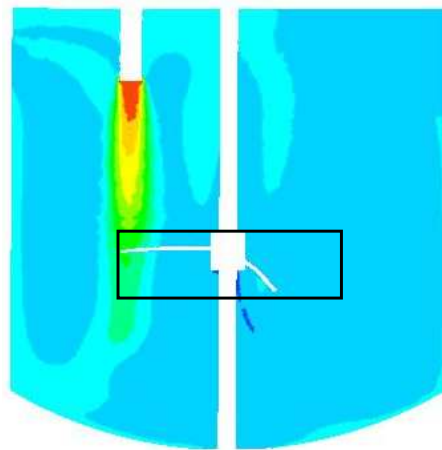
(a) MTTD, $\tau / t_m = 6.80$
Feeding-tube plane
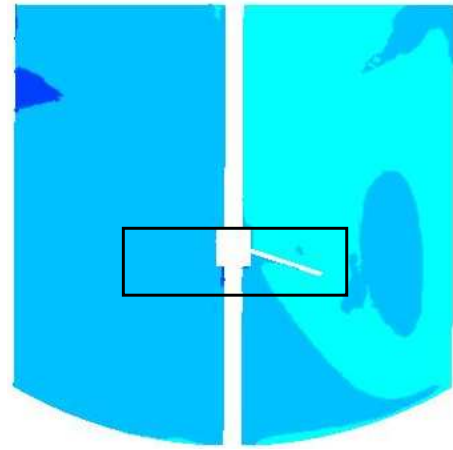
(b) MTTD, $\tau / t_m = 6.80$
90°-rotated plane

$$\overline{C^*} = 0.195, \ \sigma = 0.063$$
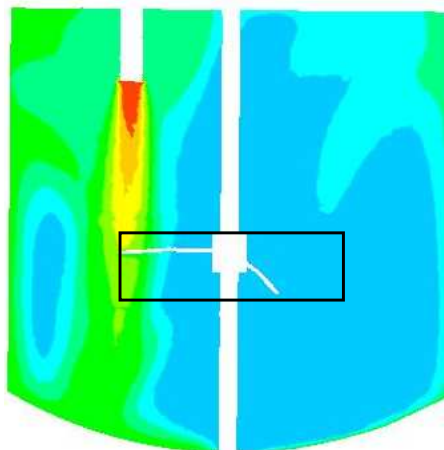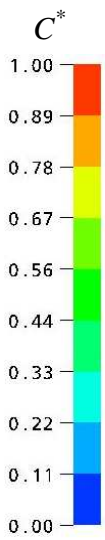
(c) MTTD, $\tau / t_m = 3.76$
Feeding-tube plane
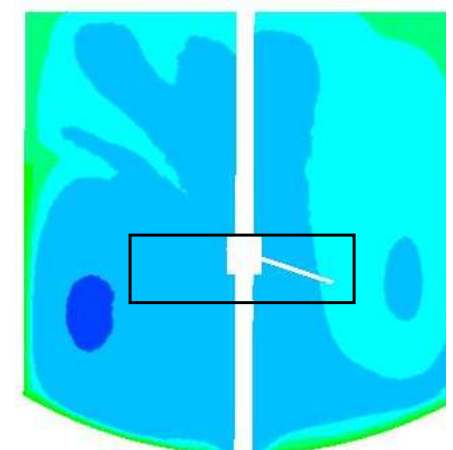
(d) MTTD, $\tau / t_m = 3.76$
90°-rotated plane

$$\overline{C^*} = 0.271, \ \sigma = 0.103$$
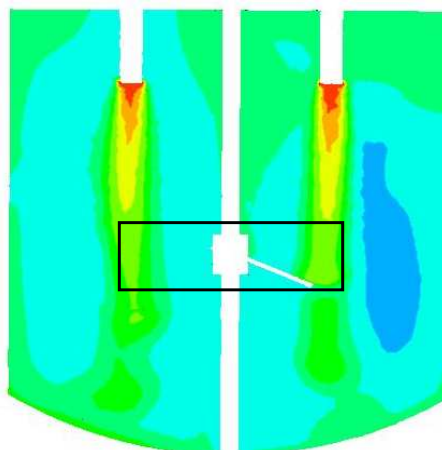
(c) MTTD (2 inlets), $\tau / t_m = 3.76$
Feeding-tube plane
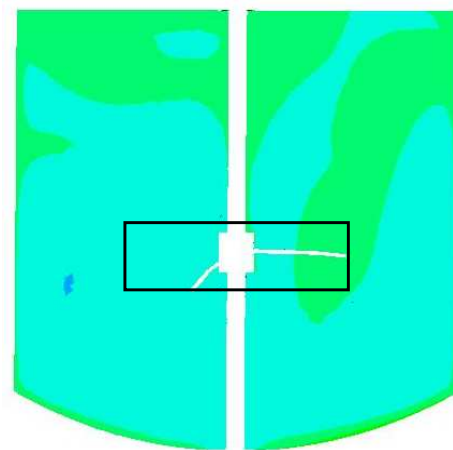
(d) MTTD (2 inlets), $\tau / t_m = 3.76$
90°-rotated plane

$$\overline{C^*} = 0.320, \ \sigma = 0.067$$

Figure 6
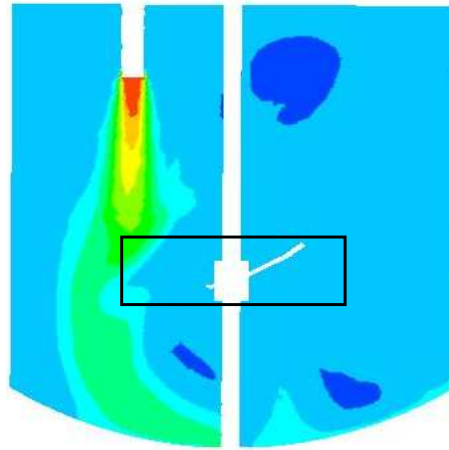
(a) MTTU, $\tau / t_m = 8.13$
Feeding-tube plane
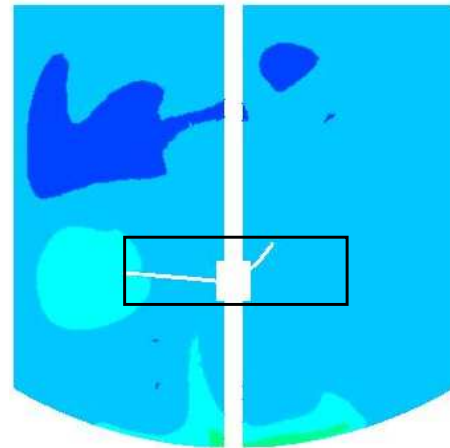
(b) MTTU, $\tau / t_m = 8.13$
90°-rotated plane

$\overline{C^*} = 0.169$, $\sigma = 0.052$
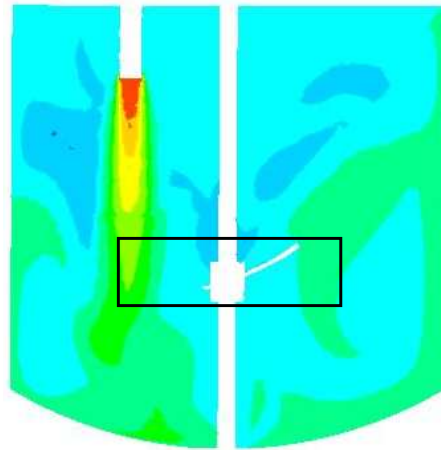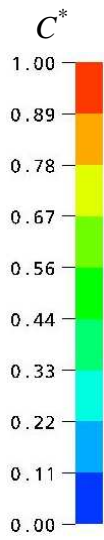
(c) MTTU, $\tau / t_m = 4.50$
Feeding-tube plane
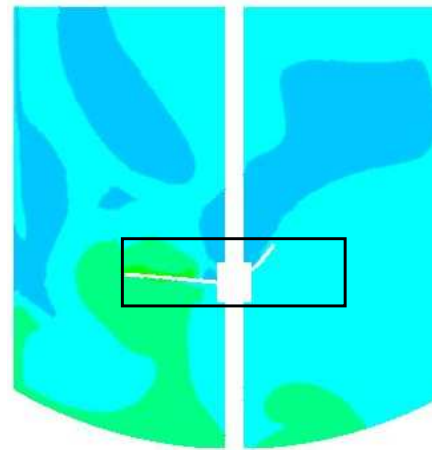
(d) MTTU, $\tau / t_m = 4.50$
90°-rotated plane

$\overline{C^*} = 0.292$, $\sigma = 0.066$

(c) MTTU (2 inlets), $\tau / t_m = 4.50$
Feeding-tube plane
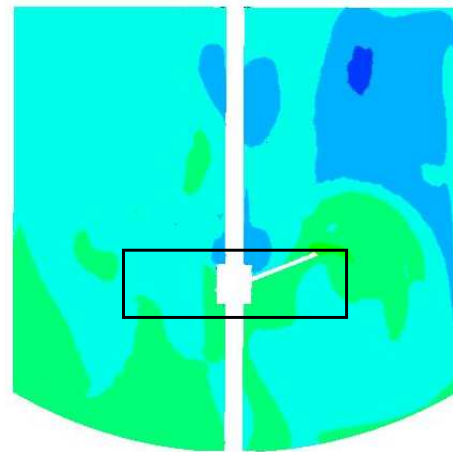
(d) MTTU (2 inlets), $\tau / t_m = 4.50$
90°-rotated plane

$\overline{C^*} = 0.288$, $\sigma = 0.060$

Figure 7
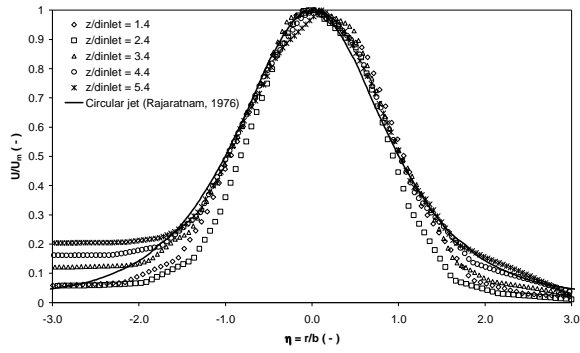
(a) MTTD, $\tau / t_m = 6.80$ (inlet over blade)
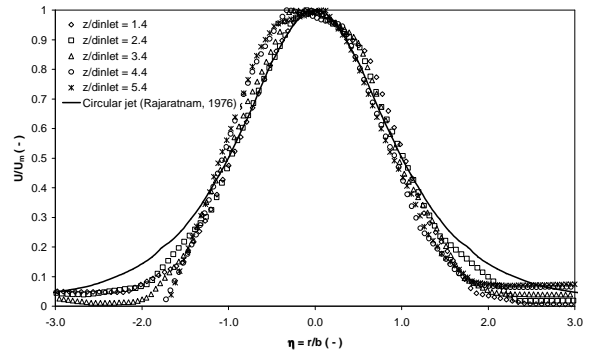
(b) MTTU, $\tau / t_m = 8.13$ (inlet over blade)
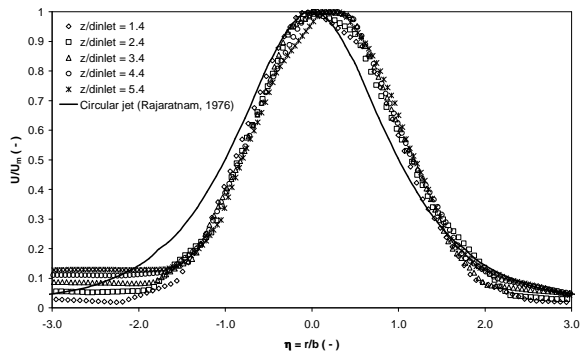
(c) MTTD $\tau / t_m = 3.76$ (inlet over blade)
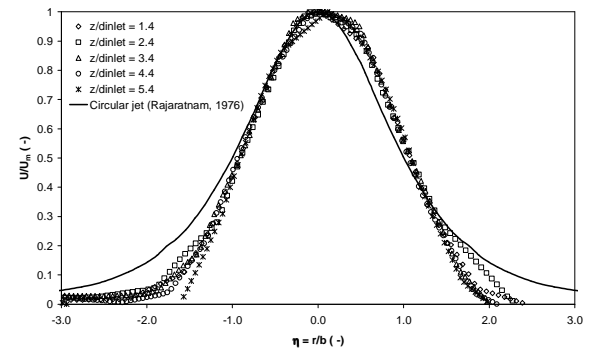
(d) MTTU $\tau / t_m = 4.50$ (inlet over blade)
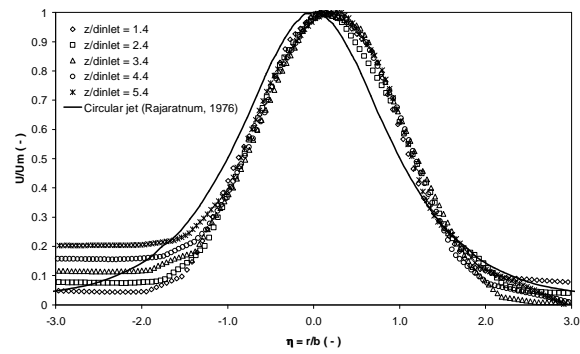
(e) MTTD 2 inlets, $\tau / t_m = 3.76$, (inlet over blade)
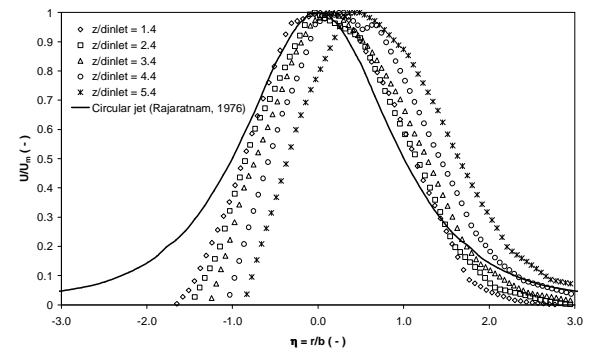
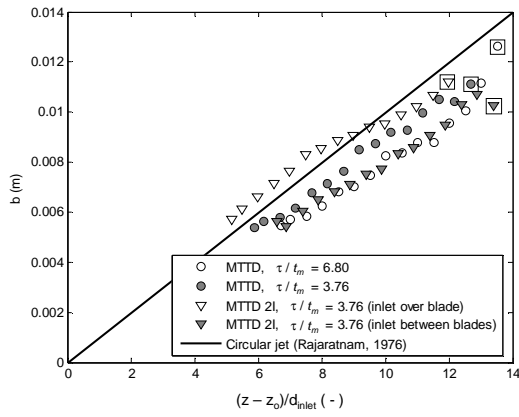(f) MTTU 2 inlets, $\tau / t_m = 4.50$, (inlet over blade)
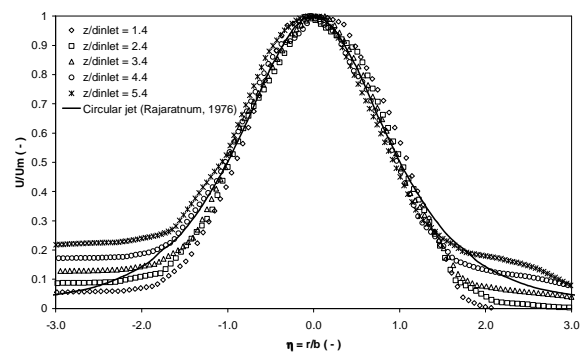
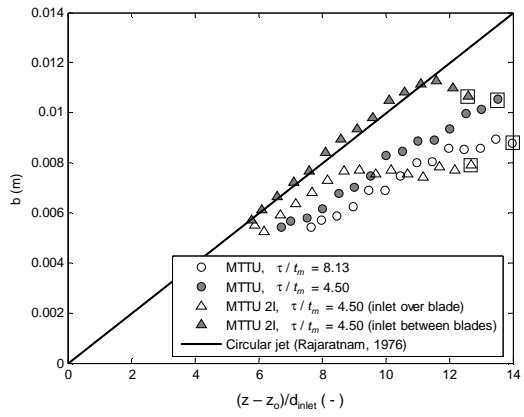(g) MTTD 2 inlets, $\tau / t_m = 3.76$, (inlet between blades)
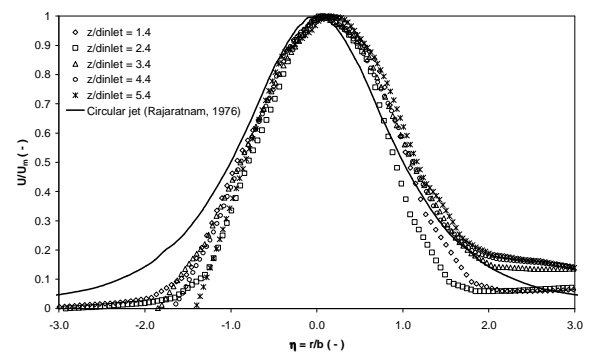
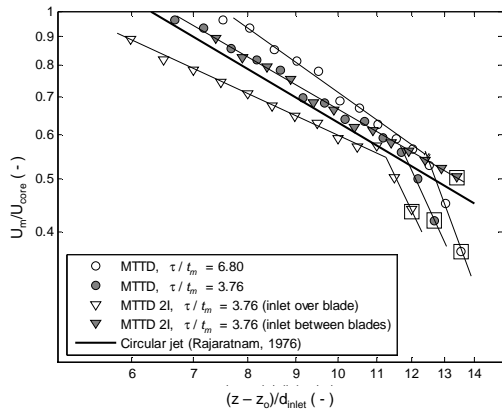(h) MTTU 2 inlets, $\tau / t_m = 4.50$, (inlet between blades)

Figure 8

(a)
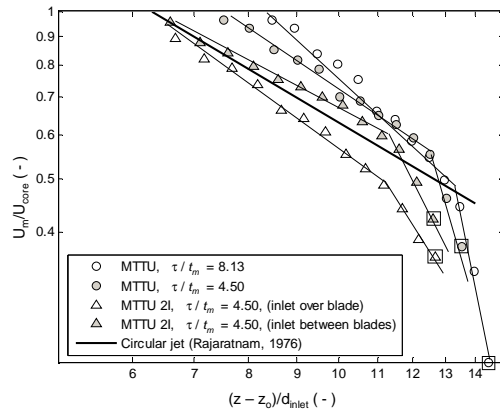
(b)

(c)

(d)

Figure 9